The FEBS Journal

FEBS PRESS science publishing by scientists

Dynamics of internalization and recycling of the prometastatic membrane type 4 matrix metalloproteinase (MT4-MMP) in breast cancer cells

Alice Truong[1], Cassandre Yip[1], Alexandra Paye[1], Silvia Blacher[1], Carine Munaut[1], Christophe Deroanne[2], Agnès Noel[1] and Nor Eddine Sounni[1]

1 Laboratory of Tumor and Development Biology, Groupe Interdisciplinaire de Génoprotéomique Appliquée-Cancer (GIGA-Cancer), University of Liège, Belgium

2 Laboratory of Connective Tissues Biology, GIGA-Cancer, University of Liège, Belgium

Keywords

breast cancer cells; endocytosis; matrix metalloproteinase; protein–protein interaction; trafficking

Correspondence

N. E. Sounni, Laboratory of Tumor and Development Biology, University of Liège, Tour de Pathologie (B23), Sart-Tilman, B-4000 Liège, Belgium

Fax: +32 43662936

Tel: +32 43662570

E-mail: nesounni@ulg.ac.be

(Received 2 June 2015, revised 3 December 2015, accepted 10 December 2015)

doi:10.1111/febs.13625

Membrane type 4 matrix metalloproteinase (MT4-MMP) [matrix metalloproteinase (MMP) 17] is a GPI-anchored membrane-type MMP expressed on the cell surface of human breast cancer cells. In triple-negative breast cancer cells, MT4-MMP promotes primary tumour growth and lung metastases. Although the trafficking and internalization of the transmembrane membrane type 1 MMP have been extensively investigated, little is known about the regulatory mechanisms of the GPI-anchored MT4-MMP. Here, we investigated the fate and cellular trafficking of MT4-MMP by analysing its homophilic complex interactions, internalization and recycling dynamics as compared with an inert form, MT4-MMP-E249A. Oligomeric and dimeric complexes were analysed by cotransfection of cells with FLAG-tagged or Myc-tagged MT4-MMP in reducing and nonreducing immunoblotting and coimmunoprecipitation experiments. The trafficking of MT4-MMP was studied with an antibody feeding assay and confocal microscopy analysis or cell surface protein biotinylation and western blot analysis. We demonstrate that MT4-MMP forms homophilic complexes at the cell surface, and internalizes in early endosomes, and that some of the enzyme is either autodegraded or recycled to the cell surface. Our data indicate that MT4-MMP is internalized by the clathrin-independent carriers/GPI-enriched early endosomal compartments pathway, a mechanism that differs from that responsible for the internalization of other membrane-type MMP members. Although MT4-MMP localizes with caveolin-1, MT4-MMP internalization was not affected by inhibitors of caveolin-1 or clathrin endocytosis pathways, but was reduced by CDC42 or RhoA silencing with small interfering RNA. We provide a new mechanistic insight into the regulatory mechanisms of MT4-MMP, which may have implications for the design of novel therapeutic strategies for metastatic breast cancer.

Abbreviations

CAV-1, caveolin-1; CHC-1, clathrin heavy chain 1; CLIC/GEEC, clathrin-independent carriers/GPI-enriched early endosomal compartments; DMEM, Dulbecco's modified Eagle's medium; EEA1, early endosome antigen 1; FACS, fluorescence-activated cell sorting; IP, immunoprecipitation; MESNA, 2-mercaptoethane sulfonic acid; MMPI, matrix metalloproteinase inhibitor; MMP, matrix metalloproteinase; MT1-MMP, membrane type 1 matrix metalloproteinase; MT4-MMP, membrane type 4 matrix metalloproteinase; MT6-MMP, membrane type 6 matrix metalloproteinase; MT-MMP, membrane-type matrix metalloproteinase; NS, not significant; SBS, Soerensen Buffer; SEM, standard error of the mean; siRNA, small interfering RNA; TIMP, tissue inhibitor of metalloproteinase; WT, wild-type.

Introduction

Matrix metalloproteinase (MMP) activity is strictly regulated in normal tissue, and proteolytic events are fine-tuned within spatiotemporal windows that maintain normal physiological function. In pathological conditions, uncontrolled MMP activity leads to tissue damage in numerous diseases, such as rheumatoid arthritis, scleroderma, aneurism rupture, and cancer invasion and metastases [1–4]. MMP activity is regulated through various mechanisms, including activation by prodomain cleavage and inhibition by physiological inhibitors [tissue inhibitor of MMP (TIMP)] [5–7]. MMP complex formation constitutes another mechanism of MMP regulation. For instance, the activities of MMP9 [8], MMP2 [9] and membrane type 1 MMP (MT1-MMP) [10] can be regulated by the formation of homodimers at the cell surface. The specific localization of some MMPs at the cell membrane allows the MMPs to contribute to the shedding or cleavage of cell surface receptors and regulation of intracellular signalling [11–15]. These membrane-type MMPs (MT-MMPs) are classified into two subgroups [16–18]: (a) transmembrane MMPs, which contain a transmembrane domain, and include MT1-MMP (MMP14), membrane type 2 MMP (MMP16), membrane type 3 MMP (MMP15), and membrane type 5 MMP (MMP24); and (b) GPI-anchored MMPs, including membrane type 4 MMP (MT4-MMP) (MMP17) and membrane type 6 MMP (MT6-MMP) (MMP25). In addition to the ability of MT-MMPs to degrade a plethora of extracellular substrates, including extracellular matrix components, growth factors, cytokines, and chemokines [5,19,20], new roles have been assigned to MT-MMPs as key mediators of leukocyte function and the immune response [21]. Recent advances include the appreciation of a nonproteolytic function of MT-MMPs leading to cell migration, signalling, and proliferation [22–24].

The availability and stability of MT-MMPs at the cell surface are tightly regulated by their trafficking, internalization, and recycling. Although the internalization and trafficking of MT1-MMP, membrane type 2 MMP and membrane type 3 MMP are well documented, little is known about the fate of the GPI-anchored MT-MMPs (MT4-MMP and MT6-MMP) [18]. Homophilic interactions of MT1-MMP are widely recognized as being crucial for its stability and ability to activate proMMP2 and exert collagenolytic activity [25–27]. Such interactions between two MT1-MMP molecules involve either covalent intermolecular interactions through disulfide bridges of cysteines [28,29] or noncovalent interactions through the MT1-MMP hemopexin domain [30,31]. In GPI-anchored MT4-MMP and MT6-MMP, homophilic interactions have been reported to involve cysteines in the stem regions of these molecules. However, the importance of MT4-MMP homophilic interactions for enzyme internalization and stability, and the role of the catalytic function of MT4-MMP, are unclear. MT4-MMP has recently emerged as a key driver in breast cancer growth and metastasis *in vivo* [32–34]. Proangiogenic and prometastatic effects of MT4-MMP can be abrogated by an inactivating mutation (E249A) in the catalytic site of the enzyme [32]. In addition to its proteolytic activity, MT4-MMP affects breast cancer cell proliferation by interacting with epidermal growth factor receptor and enhancing its activation in response to ligand [24]. Superimposition of MT4-MMP and epidermal growth factor receptor has been observed in human triple-negative breast cancer specimens [24]. Our recent data revealed both proteolytic and nonproteolytic functions of MT4-MMP, and targeting of these functions to interfere with different steps in cancer progression (including tumour cell proliferation, angiogenesis, cancer invasion, and metastatic dissemination) is warranted. In this context, a better understanding of MT4-MMP fate at the cell surface and intracellular trafficking of MT4-MMP in cancer cells is essential for the design of efficient strategies to counteract its protumorigenic and prometastatic effects [35].

Here, we demonstrate that MT4-MMP forms oligomers and colocalizes with caveolin-1 (CAV-1) at the cell surface. After MT4-MMP internalization, which occurs within 45 min, some of the enzyme is intracellularly autodegraded, whereas the remaining intact MT4-MMP proteins are recycled to the cell surface. Our study provides evidence for the involvement of the clathrin-independent carriers/GPI-enriched early endosomal compartments (CLIC/GEEC) pathway in MT4-MMP internalization, highlighting unique features of MT4-MMP among membrane-associated MMPs.

Results

MT4-MMP is internalized and autodegraded

The internalization dynamics of MT4-MMP were investigated in MDA-MB-231 cells stably transfected with: (a) the control vector pcDNA3-neo (control plasmid); (b) full-length active human MT4-MMP cDNA [MT4-wild-type (WT)]; or (c) cDNA of the inert form of MT4-MMP containing a point mutation (E249A) in its catalytic domain (MT4-E249A). All MT4-MMP constructs contained a FLAG tag in the hinge region (Fig. 1A). MT4-MMP expression in transfected cells

was analysed by RT-PCR (Fig. 1B) and western blotting under reducing conditions, with antibodies against FLAG and MT4-MMP (Fig. 1C,D). A cell surface protein biotinylation assay was performed to analyse the amount of internalized MT4-MMP at different time points (Fig. 2A). After biotinylation, cells were incubated at 37 °C for different times (15, 30, 45 and 60 min), and cell surface biotin was removed with 2-mercaptoethane sulfonic acid (MESNA). Biotinylated proteins in the total cell lysates were pulled down with streptavidin beads, and analysed by western blotting with an antibody against FLAG. As expected, MT4-WT and MT4-E249A were found at the cell surface, and no enzyme was detected after treatment with MESNA at time 0 (Fig. 2B). MT4-WT and MT4-E249A were detected in cells 15 min after cell treatment with MESNA and incubation at 37 °C, and the internalization of MT4-E249A was enhanced after 45–60 min. MT4-WT was less abundant than MT4-E249A at any time point in the MESNA condition,

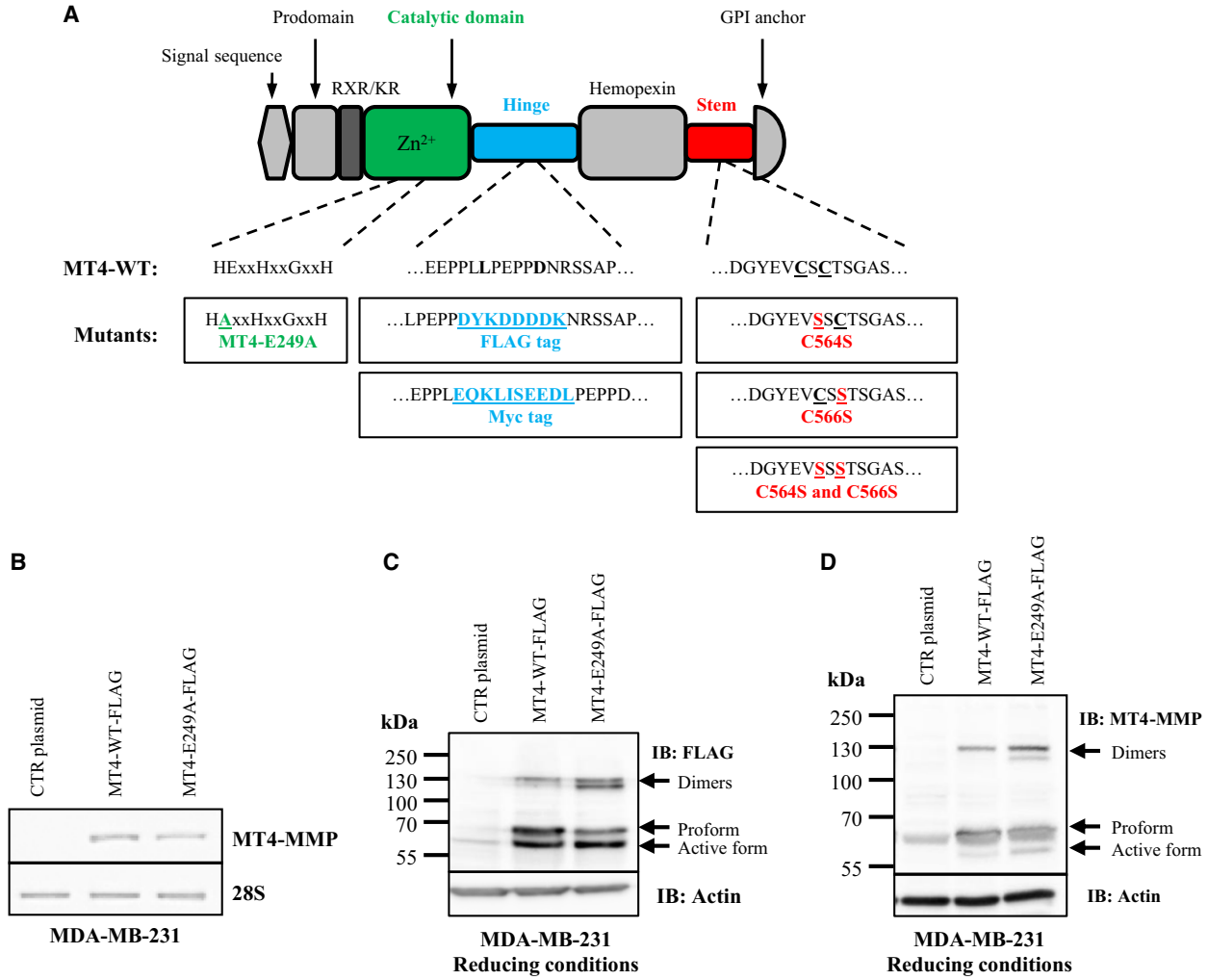

Fig. 1. Generation of MT4-MMP constructs and stably transfected MDA-MB-231 cells. (A) Schematic illustration of MT4-MMP cDNA constructs. Full-length MT4-MMP contains a signal sequence, a prodomain, a furin cleavage site (RXR/KR), a catalytic domain, a hinge region, a hemopexin-like domain ('Hemopexin'), a stem region, and a GPI anchor. A Myc or FLAG tag was inserted into MT4-MMP cDNA (MT4-WT-FLAG or MT4-WT-Myc) to allow detection by antibody against Myc or FLAG. The replacement of the glutamic acid at position 249 with alanine in the highly conserved domain HExxHxxGxxH generates an inactive enzyme (MT4-E249A). FLAG or Myc was also inserted into this inert form (MT4-E249A-FLAG or MT4-E249A-Myc). Two substitutions of cysteine with serines were also generated (C564S and C566S) as single or combined mutations. (B–D) MT4-MMP expression was analysed by RT-PCR (B) and western blotting for MT4-MMP with antibody against FLAG (C) or MT4-MMP (D) in cell lysates from MDA-MB-231 cells stably transfected with control vector pcDNA3-neo (CTR plasmid), full-length tagged MT4-MMP (MT4-WT-FLAG), or the inert tagged form (MT4-E249A-FLAG). 28S rRNA and actin were used as loading controls for RT-PCR and western blot analysis, respectively. IB, immunoblotting.

suggesting either lack of internalization of the active form or possible degradation during its internalization. To assess this possibility, MT4-WT cells were incubated with the broad-spectrum MMP inhibitor (MMPI) BB94 (20 μM), and subjected to the biotinylation assay. Interestingly, treatment with BB94 increased the amounts of internalized MT4-WT detected at the different time points (Fig. 2B). These data were confirmed with an antibody feeding assay and confocal microscopy analysis followed by computerized quantification of the internalized MT4-MMP (see Experimental procedures). In MT4-E249A cells, internalized MT4-MMP was visible as green spots in the cytoplasm. In the absence of BB94, only a few spots were detectable in MT4-WT cells, even after 60 min. In contrast, MT4-MMP degradation was completely prevented by the MMPI (Fig. 2C). Computerized quantification of internalized MT4-MMP (51–97 cells) after 60 min in the presence or absence of MMPI (BB94) confirmed the restoration of the active WT form to a similar level as the inert form (Fig. 2D). These data demonstrate that MT4-MMP is internalized and partially autodegraded, a process that is prevented by the inactivation of its catalytic domain or treatment with BB94. Having obtained similar effects with pharmacological MMP inhibition and mutation-driven catalytic inactivation, we thereafter compared the fate of WT and catalytically inert MT4-MMP forms expressed by stably transfected cells in the absence of MMPIs.

MT4-MMP is internalized in early endosomes and recycled to the cell surface

The intracellular trafficking of MT4-MMP was next investigated with an antibody feeding assay and immunofluorescent staining of endosomes. MT4-MMP (marked in green) was found to be associated with early endosome antigen 1 (EEA1)-positive endosomes (marked in red) 10 min after the internalization of MT4-MMP from the cell surface (Fig. 2E). This association was even more pronounced at 30 min and 60 min in both MT4-WT and MT4-E249A cells, as shown by yellow spots.

The MT4-MMP internalization prompted us to assess whether recycling of the enzyme that was not degraded during this process was occurring. For this purpose, and because of the partial autodegradation of MT4-MMP during its internalization, we increased the amount of protein used for the immunoprecipitation (IP) to 800 μg instead of the 600 μg used in Fig. 2B, to allow the detection of MT4-WT during its recycling. Cells were biotinylated and incubated for 45 min at 37 °C to allow the internalization of MT4-MMP, and treated with MESNA to remove all of the biotinylated proteins remaining at the cell surface. Then, a second incubation at 37 °C for 30 min allowed the recycling of proteins to the cell membrane, and a second treatment with MESNA was performed to cleave all of the biotinylated MT4-MMP re-exposed at the cell surface (Fig. 3A). The pulldown of biotinylated proteins in the total cell lysates and western blotting revealed that MT4-MMP was recycled to the cell surface by 30 min after its internalization in both MT4-WT and MT4-E249A cells (Fig. 3B). The difference between MESNA-treated and untreated cells at 30 min represents the amount of protein recycled to the cell surface. Similarly to the data in Fig. 2B, the density of the total amount of internalized active form (lane 6 versus lane 5) was lower than that of the inert form (lane 2 versus lane 1). The density ratios of the recycled active (lane 8 versus lane 6) and inert (lane 4 versus lane 2) forms were similar. These data demonstrate that intact MT4-MMP is recycled to the cell surface, and that the inactivation mutation E249A increased its stability but did not affect its internalization and recycling dynamics.

MT4-MMP forms homophilic complexes

To investigate in detail the homophilic complexes formed by MT4-MMP, we generated single and double mutations, i.e. C564S and C566S, in the stem regions of MT4-WT and MT4-E249A containing a Myc or FLAG tag inserted into the hinge region (Fig. 1A). MT4-MMP homophilic complexes were analysed by western blotting under nonreducing conditions in COS-1 and MDA-MB-231 cells transfected with MT4-WT and MT4-E249 cDNA (Fig. 4A). Under nonreducing conditions, MT4-WT and MT4-E249A were found as monomers (65-kDa species), dimers (130-kDa species), and many oligomers (260-kDa species). Next, COS-1 cells were double-transfected with FLAG-tagged and Myc-tagged MT4-WT, and this was followed by IP of Myc-tagged proteins and western blotting for the FLAG tag under reducing conditions (Fig. 4B). MT4-MMP–FLAG was immunoprecipitated with MT4-MMP–Myc, which confirmed the formation of homophilic complexes of the enzyme. To determine whether the binding of TIMP2 or MMPIs to the catalytic domain of MT4-MMP could disturb these interactions, COS-1 cells were double-transfected with MT4-WT and MT4-E249A containing either a FLAG or Myc tag, and incubated with BB94, GM6001, or TIMP2; this was followed by IP for Myc and western blotting for

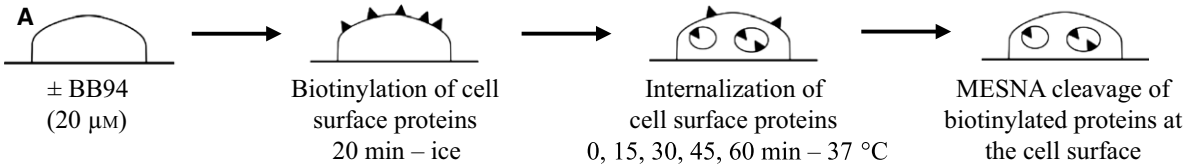
A
± BB94
(20 μM)
Biotinylation of cell
surface proteins
20 min – ice
Internalization of
cell surface proteins
0, 15, 30, 45, 60 min – 37 °C
MESNA cleavage of
biotinylated proteins at
the cell surface

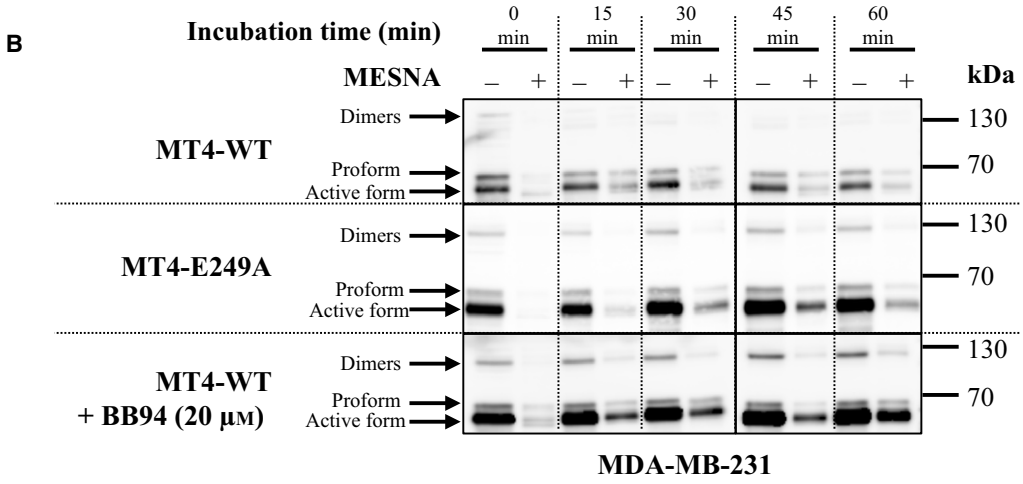
B
Incubation time (min)
0 min
15 min
30 min
45 min
60 min
MESNA
– + – + – + – + – +
kDa
MT4-WT
Dimers
Proform
Active form
130
70
MT4-E249A
MT4-WT
+ BB94 (20 μM)
MDA-MB-231

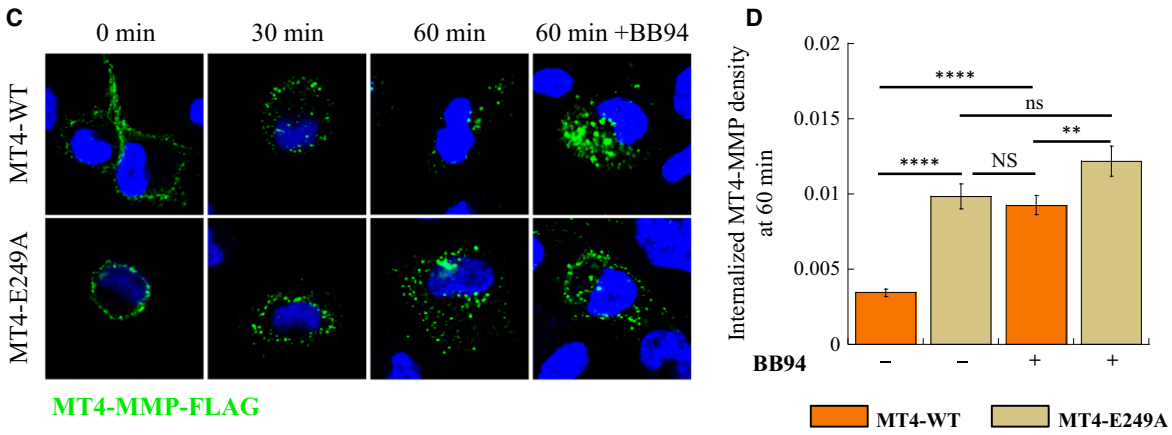
C
0 min
30 min
60 min
60 min +BB94
MT4-WT
MT4-E249A
MT4-MMP-FLAG
D
Internalized MT4-MMP density
at 60 min
0.02
0.015
0.01
0.005
0
****
ns
**
****
NS
BB94
– – + +
MT4-WT
MT4-E249A

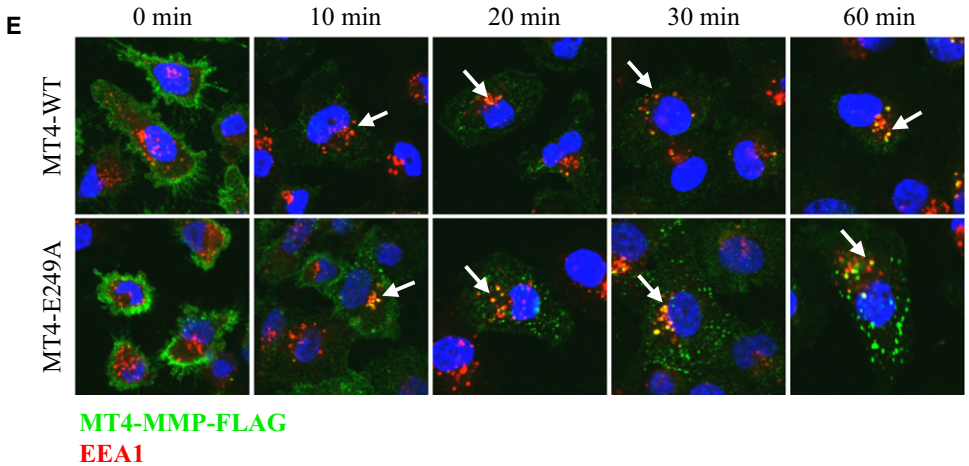
E
0 min
10 min
20 min
30 min
60 min
MT4-WT
MT4-E249A
MT4-MMP-FLAG
EEA1

Fig. 2. MT4-MMP is internalized in early endosomes and autodegraded. (A) Schematic representation of the internalization assay of MT4-MMP in MT4-WT-expressing and MT4-E249A-expressing MDA-MB-231 cells. After cell surface biotinylation (black spots), the cells were incubated at 37 °C for different times to allow internalization of cell surface proteins. Treatment with MESNA removed biotin remaining at the cell surface. The cells had previously been incubated or not with BB94 (20 μM). (B) Detection of internalized (+ MESNA) or total (– MESNA) biotinylated MT4-MMP-FLAG or MT4-E249A-FLAG at different time points in MDA-MB-231 cells by western blot analysis with an antibody against FLAG. MT4-MMP-FLAG cells were incubated or not with BB94. (C) Internalization dynamics of MT4-WT and its inert form MT4-E249A in MDA-MB-231 cells after 0, 30 and 60 min determined by an antibody feeding assay with an Alexa Fluor 488-coupled antibody against FLAG (green). Cells were incubated or not with BB94 24 h before the assay. (D) Computerized quantification of confocal images representing internalized MT4-WT and MT4-E249A in MDA-MB-231 cells at 60 min in the presence or absence of BB94. The data and statistical analysis in (D) are representative of three independent experiments ($n = 3$) performed in biological triplicates. Data are presented as the mean (± SEM) of the ratio between the intracellular staining areas and the cell surface (internalized MT4-MMP density). Wilcoxon–Mann–Whitney tests were performed. NS, $P > 0.05$; $^{**}P \leq 0.01$; $^{****}P \leq 0.0001$. (E) Antibody feeding assay of MT4-MMP combined with coimmunofluorescence with EEA1 performed in MT4-WT-expressing or MT4-E249A-expressing MDA-MB-231 cells at the indicated time points. MT4-MMP was labelled with an antibody against FLAG as green spots, and EEA1 was detected as red spots. Internalized MT4-MMP colocalized with EEA1-positive endocytic markers in MDA-MB-231 cells as shown by yellow spots (white arrows). The cells were observed under a confocal microscope and using a 60X objective.

FLAG under reducing conditions (Fig. 4C). FLAG-tagged MT4-WT and MT4-E249A were immunoprecipitated with the Myc-tagged enzyme in the absence or presence of DMSO, BB94, GM6001, or TIMP2. These results indicated that MT4-MMP oligomerization does not require an intact catalytic domain and is not impaired by the binding of an inhibitor. Intriguingly, a 130-kDa band of MT4-MMP was detectable under reducing conditions after the IP experiments; this band may correspond to a dimer formed by non-

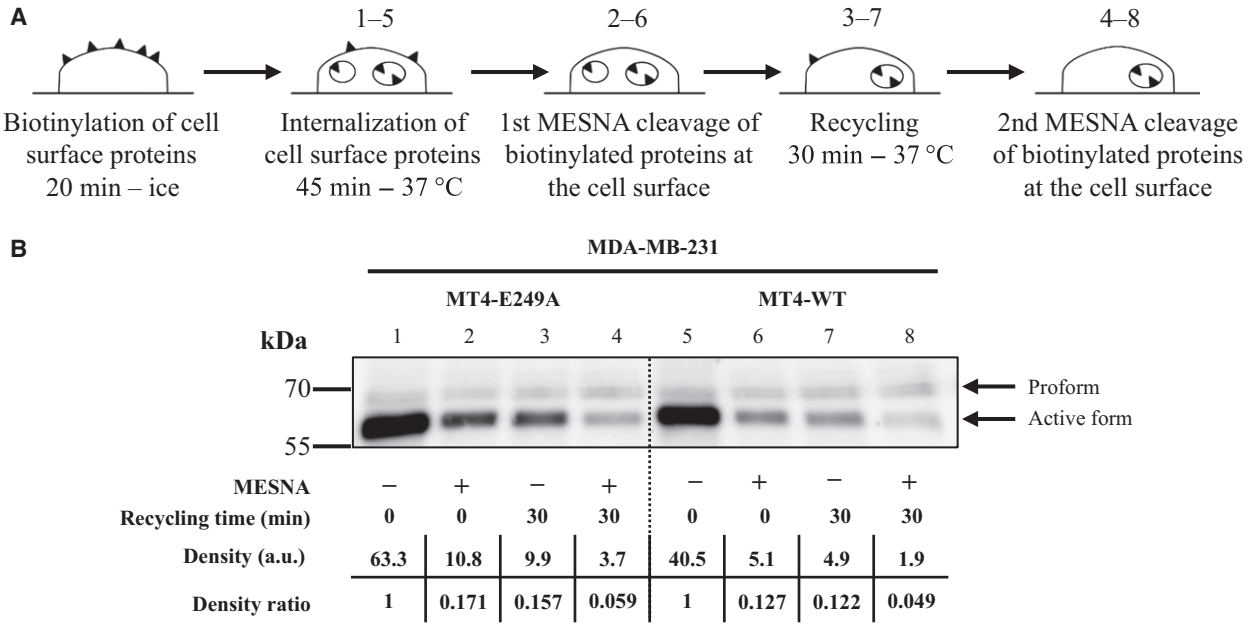

Fig. 3. MT4-MMP is recycled to the cell surface. (A) Schematic representation of the recycling assay of MT4-MMP in MT4-WT-expressing and MT4-E249A-expressing MDA-MB-231 cells. After cell surface biotinylation (black spots), the cells were incubated for 45 min at 37 °C to allow internalization of cell surface proteins. A first treatment with MESNA removed biotin remaining at the cell surface, and was followed by a second incubation at 37 °C for 30 min to allow the recycling of biotinylated enzymes. A second MESNA treatment cleaved all of the biotinylated proteins re-exposed on the surface. Protein extracts were immunoprecipitated with streptavidin beads, and separated by SDS/PAGE to analyse the expression of MT4-MMP by immunoblotting with an antibody against FLAG. Differences between the conditions with subjection or not to the second MESNA treatment determine the amount of recycled enzyme at the cell surface. (B) Western blot analysis of MT4-MMP expression after the recycling assay as described in (A). The difference between lane 3 and 4 or between lane 7 and 8 represents the amount of protein recycled to the cell surface during the second incubation at 37 °C. Densitometry quantification of western blot band is represented by arbitrary units (a.u.). The density ratio of internalized and recycled MT4-MMP is normalized to lane 1 for MT4-E249A and to lane 5 for MT4-WT.

covalent bonding of two molecules released from the large oligomeric complexes of MT4-MMP (Fig. 4A). Similar stable dimers (130 kDa) were also detected, but to a lesser extent, under reducing conditions, whereas oligomers were completely dissolved in these conditions (Figs 1C and 4B). Different antibodies directed against different epitopes, including antibody against MT4-MMP or antibody against FLAG, under reducing conditions confirmed that the 130-kDa band was specific to MT4-MMP (data not shown). Our data support the concept that MT4-MMP dimers could be held by both covalent and noncovalent bonds. The persistence of MT4-MMP oligomers in the presence of MMPIs, including BB94, GM6001, and TIMP2, was confirmed by nonreducing western blotting in MDA-MB-231 and COS-1 cells, in which MT4-MMP dimers were still observed at 130 kDa (Fig. 4D).

To test whether MT4-MMP homophilic interactions are dependent on Cys564 and/or Cys566 residues in its stem region, COS-1 cells were transfected with MT4-MMP cDNA bearing either a single mutation (C564S or C566S) or a double mutation (C564S and C566S) (Fig. 1A). Under nonreducing conditions, all forms of MT4-MMP (65-kDa monomers, 130-kDa dimers, and 260-kDa oligomers) were found in cells transfected with MT4-WT, MT4-E249A, MT4-C564S, and/or MT4-C566S constructs (Fig. 5A). Similar results were obtained in double-transfection experiments followed by IP and western blotting (Fig. 5B). MT4-FLAG-C564S, MT4-FLAG-C566S and MT4-FLAG-C564S-C566S were found to be immunoprecipitated with their respective proteins containing a Myc tag, suggesting that the homophilic interactions of MT4-MMP were not inhibited by the cysteine mutations in the stem region. However, the 130-kDa band of MT4-MMP, which was still detected under reducing conditions, was decreased by the C564S mutation but not by the C566S mutation. Double mutation of the two cysteines led to the same result as the single C564S mutation, with no additional inhibitory effects. In agreement with previous data from Sohail *et al.* [36], these data confirm the role of Cys564 in MT4-MMP homophilic interactions, but also demonstrate a possible role of other noncovalent interactions that are independent of the cysteines in the stem region.

To further analyse the effects of C564S and C566S mutations on MT4-MMP internalization, we compared the internalization of MT4-C564S-C566S with that of MT4-WT in the biotinylation assay after 45 min (Fig. 5C). Similar levels of the MT4-MMP proform (65 kDa) were found at the cell surface of COS-1 cells at time 0 without MESNA. No difference was observed between the WT form of MT4-MMP and MT4-WT-C564S-C566S after 45 min of internalization. MT4-MMP in COS-1 cells is mainly produced as inactive proform (65 kDa) that is endocytosed and found intact intracellularly, as it is protected from autodegradation. In agreement with the data in Fig. 2B, the amount of the active form (57 kDa) was lower in COS-1 cells, owing to its autodegradation during its internalization. Collectively, these data indicate that, under the experimental conditions used here, the C564S and C566S mutations did not affect MT4-MMP internalization. However, large homophilic complexes may involve other hydrophobic and polar interactions through the hemopexin domain of MT4-MMP.

MT4-MMP internalization involves the CLIC/GEEC pathway

Like most GPI-anchored proteins, MT4-MMP has been found in lipid rafts, which constitute a membrane microdomain enriched in glycosphingolipids and cholesterols [36]. This observation was confirmed by immunofluorescence and confocal microscopy analyses, which showed colocalization of MT4-MMP with CAV-1 at the cell surface (Fig. 6A). Interestingly, both

Fig. 4. MT4-MMP forms dimers and oligomers in the presence or absence of its catalytic activity. (A) Nonreducing western blot analysis of MT4-WT-FLAG and its inactive form MT4-E249A-FLAG with an antibody against FLAG in MDA-MB-231 cells stably transfected (left panel) or COS-1 cells transiently transfected (right panel) with MT4-MMP constructs or a control vector (CTR plasmid). (B) Total cell lysates from COS-1 cells double-transfected with MT4-WT-FLAG and MT4-WT-Myc constructs were immunoprecipitated with an antibody against Myc, and then blotted with an antibody against FLAG or an antibody against Myc as a loading control. The detection of FLAG after anti-Myc IP demonstrates the homophilic interaction of MT4-MMP molecules. COS-1 cells transfected with a control vector (control plasmid) or single MT4-MMP containing either a FLAG or Myc tag were used as controls for the IP. Western blots with FLAG and Myc antibody on total cell lysates from transfected cells are indicated. (C) Detection of MT4-MMP homophilic complexes in COS-1 cells double-transfected with MT4-WT-Myc and active or inactive MT4-MMP (MT4-WT-FLAG or MT4-E249A-FLAG, respectively) incubated with MMPIs (GM6001 and BB94) or TIMP2 or DMSO (used as control) for 24 h. Total cell lysates were subjected to IP with an antibody against Myc and western blotting with an antibody against FLAG. (D) Nonreducing western blot analysis of MT4-WT-FLAG with an antibody against FLAG in MDA-MB-231 and COS-1 cells transfected with MT4-MMP constructs and incubated for 24 h with control (CTR) (DMSO), MMPIs (GM6001 and BB94), or TIMP2. IB, immunoblotting.

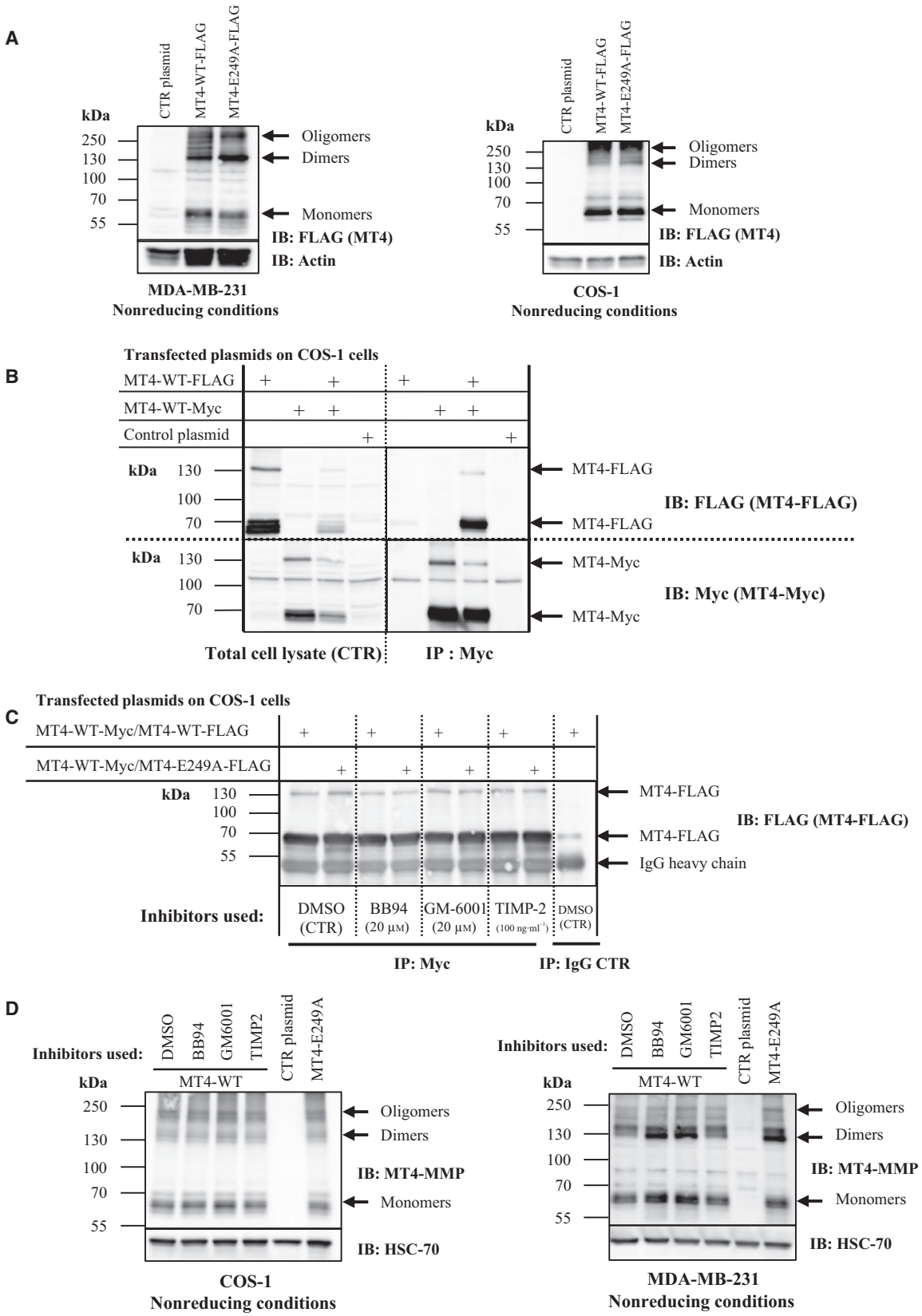
A
CTR plasmid
MT4-WT-FLAG
MT4-E249A-FLAG
kDa
250
130
100
70
55
Oligomers
Dimers
Monomers
IB: FLAG (MT4)
IB: Actin
MDA-MB-231
Nonreducing conditions
COS-1
Nonreducing conditions
B
Transfected plasmids on COS-1 cells
MT4-WT-FLAG
MT4-WT-Myc
Control plasmid
MT4-FLAG
IB: FLAG (MT4-FLAG)
MT4-Myc
IB: Myc (MT4-Myc)
Total cell lysate (CTR)
IP : Myc
C
Transfected plasmids on COS-1 cells
MT4-WT-Myc/MT4-WT-FLAG
MT4-WT-Myc/MT4-E249A-FLAG
IgG heavy chain
Inhibitors used:
DMSO (CTR)
BB94 (20 μM)
GM-6001 (20 μM)
TIMP-2 (100 ng·ml⁻¹)
IP: Myc
IP: IgG CTR
D
DMSO
BB94
GM6001
TIMP2
MT4-WT
MT4-E249A
IB: MT4-MMP
IB: HSC-70
COS-1
Nonreducing conditions
MDA-MB-231
Nonreducing conditions

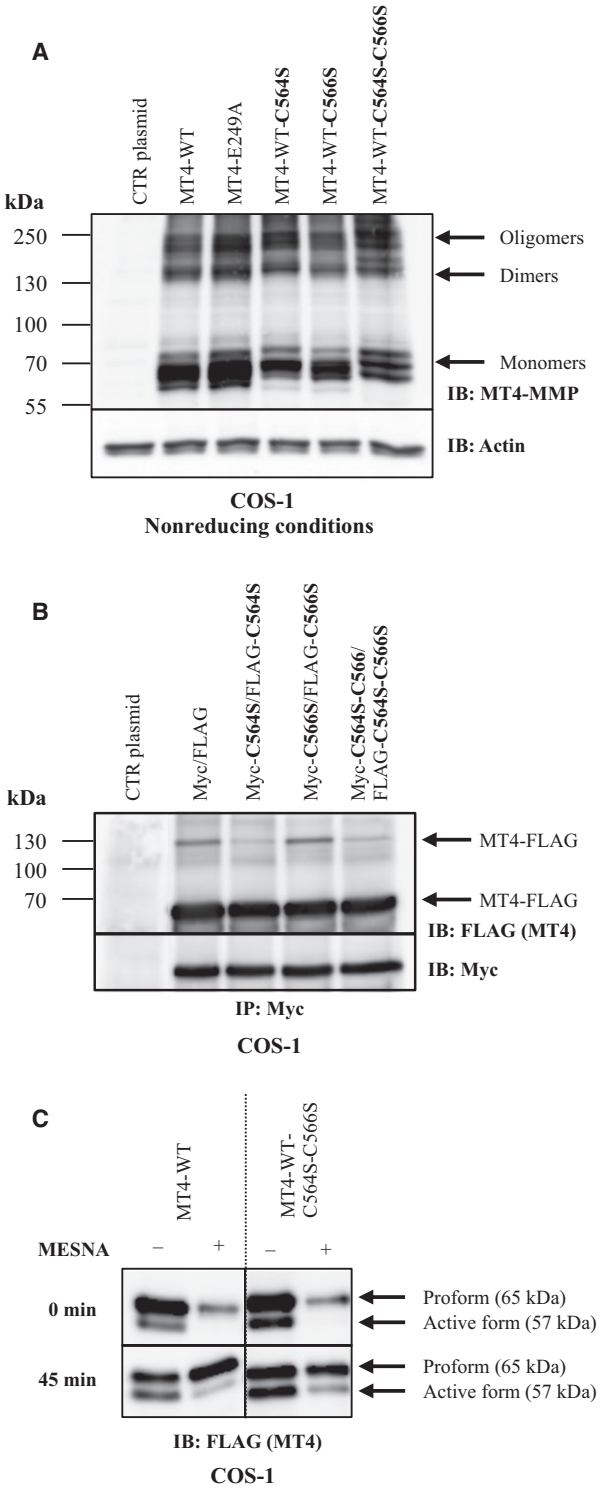

Fig. 5. Mutation of cysteines in the stem region of MT4-MMP does not affect its oligomerization. (A) Nonreducing western blot analysis of MT4-MMP in COS-1 cells transiently transfected with a control vector (CTR plasmid), MT4-WT-FLAG, MT4-E249A-FLAG, or MT4-WT containing the C564S and/or C566S mutations and containing a FLAG or Myc tag insertion. MT4-MMP molecules containing the single or double mutations C564S and C566S were detected as monomers, dimers, and oligomers. (B) Total cell lysates from COS-1 cells transfected with the two MT4-MMP FLAG and Myc constructs containing the C564S and/or C566S mutations were immunoprecipitated with an antibody against Myc and blotted with an antibody against FLAG. Western blotting against Myc was used as a loading control for the IP. (C) Detection of internalized (+ MESNA) or total (– MESNA) biotinylated MT4-WT and its mutated form containing the double mutation C564S and C566S in COS-1 cells after cell surface biotinylation and incubation for 45 min at 37 °C. IB, immunoblotting.

MT4-WT and MT4-E249A were found to colocalize with CAV-1, as shown by yellow spots in MDA-MB-231 cells (Fig. 6A). In contrast, no association of MT4-MMP with clathrin was detected in these cells (Fig. 6B). Despite the fact that MT4-MMP colocalized with CAV-1, incubating the cells with multiple concentrations (5 $\mu g \cdot mL^{-1}$ and 10 $\mu g \cdot mL^{-1}$) of filipin III, a caveolae pathway inhibitor, before the antibody feeding assay failed to influence MT4-WT or MT4-E249A internalization (Fig. 6C). Similarly, treatment with a clathrin inhibitor, chlorpromazine (5 $\mu g \cdot mL^{-1}$), did not block MT4-MMP internalization (Fig. 6C). Computerized quantification of the MT4-MMP internalization density (40–60 cells) did not reveal any effect of chlorpromazine or filipin III in MT4-WT and MT4-E249A cells (Fig. 6D). We then hypothesized that MT4-MMP may utilize the CLIC/GEEC pathway. This pathway is commonly used for GPI-anchored protein endocytosis, and is dependent on Rho GTPases, such as CDC42 and RhoA. We first silenced CDC42 with small interfering RNA (siRNA), and performed the antibody feeding assay to track MT4-MMP internalization. The expression of CDC42 was reduced by 80% in cells transfected with CDC42 siRNA in comparison with control scrambled siRNA (Fig. 7A). MT4-MMP internalization in CDC42 siRNA and control cells was followed by incubation with an antibody against FLAG and a cell membrane tracker (Fig. 7B). This antibody feeding assay revealed that MT4-MMP green spots initially localized at the cell surface were found in the cytoplasm within 30 min in the control cells (scrambled siRNA). In contrast, only few cytoplasmic spots of MT4-MMP were observed in CDC42-silenced cells, revealing impaired MT4-MMP internalization. Quantification analysis of the antibody feeding assay experiments (74–77 cells) confirmed a significant reduction in MT4-MMP internalization by CDC42 siRNA as compared with scrambled siRNA (Fig. 7C). However, MT4-MMP did not accumulate at the cell surface upon CDC42 silenc-

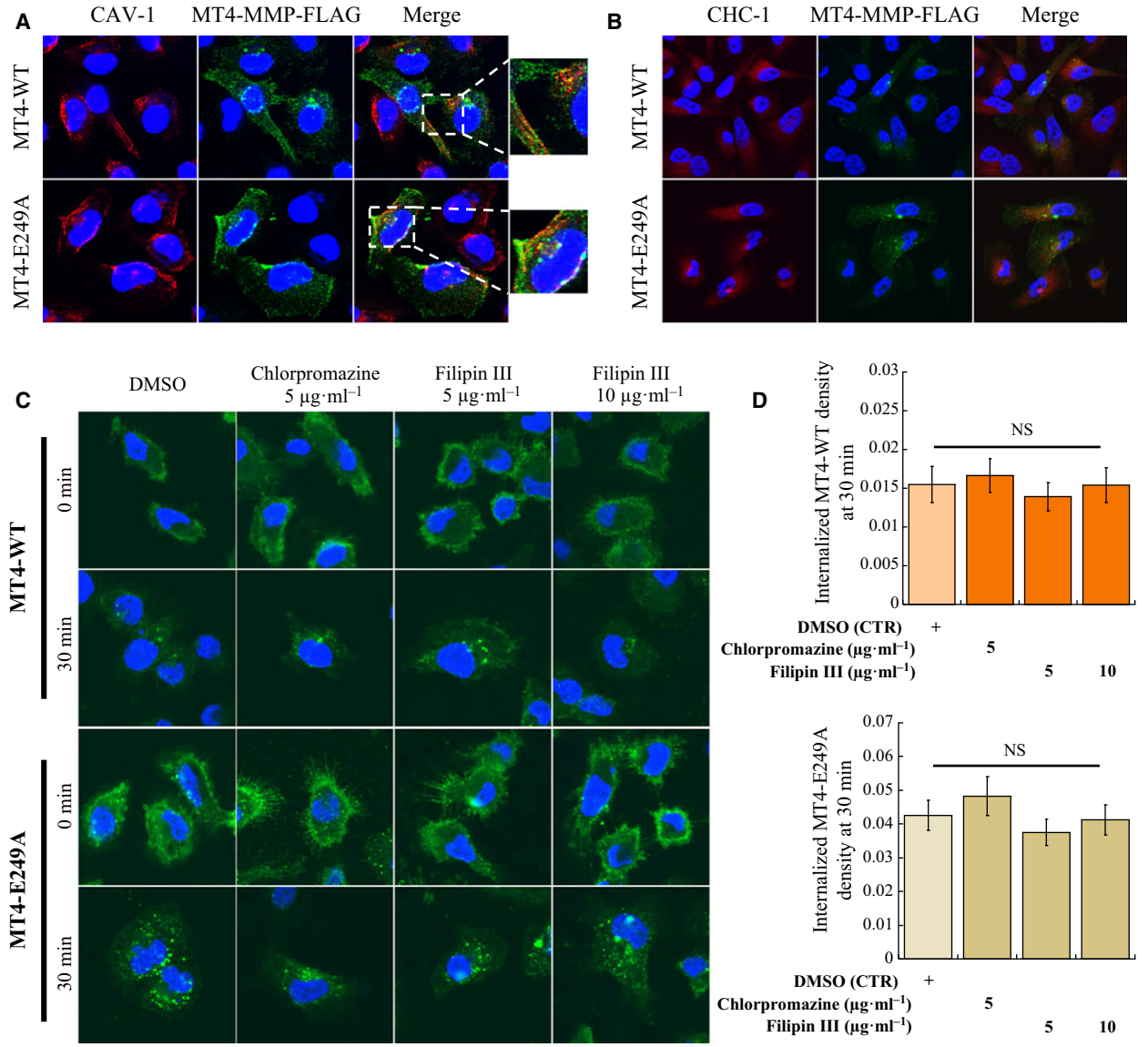

Fig. 6. MT4-MMP endocytosis is not clathrin-dependent or caveolin-dependent. (A, B) Immunofluorescence of MT4-MMP with an antibody against FLAG (green) and CAV-1 (A) or clathrin (CHC-1) (B) (red) in MDA-MB-231 cells expressing MT4-WT-FLAG or MT4-E249A-FLAG. High magnification in (A): the dashed area shows colocalization (yellow spots) of MT4-MMP with CAV-1 at the cell surface. (C) Antibody feeding assay of MT4-WT-FLAG-expressing or MT4-E249A-FLAG-expressing cells with an antibody against FLAG and incubation with a caveolin inhibitor, filipin III, at 5 µg·mL^{-1} and 10 µg·mL^{-1} or with a clathrin inhibitor, chlorpromazine, at 5 µg·mL^{-1} did not affect the internalization of MT4-MMP (MT4-WT) or its inactive form (MT4-E249A). The cells were observed under confocal microscope and using a 60X objective. (D) Computerized quantification of internalized MT4-WT and MT4-E249A in MDA-MB-231 cells at 30 min. Data and statistical analysis are representative of three independent experiments ($n = 3$) performed in biological triplicates. Data are presented as the mean (± SEM) of the ratio between the intracellular staining areas and the cell surface (internalized MT4-MMP density). For statistical analysis, Wilcoxon–Mann–Whitney tests were performed. NS, $P > 0.05$. CTR, control.

ing, suggesting that the enzyme may have been subjected to degradation and/or shedding. To check this hypothesis, internalization of the inert form MT4-E249A was followed with an antibody feeding assay in cells transfected with scrambled or CDC42 siRNA (Fig. 7A). Confocal immunofluorescence image and quantification analysis of the MT4-E249A remaining at the cell surface (62–85 cells) after 30 min of incubation confirmed the inhibitory effect of CDC42 siRNA on MT4-MMP internalization (Fig. 7D,E). After 30 min of incubation, inactive MT4-E249A was well internalized and its level at the cell surface was very low in

Fig. 7. MT4-MMP is dependent on CLIC/GEEC pathway endocytosis. (A) Western blot analysis of CDC42 in MT4-MMP-expressing MDA-MB-231 cells incubated with CDC42 or scrambled siRNA (Scr). Actin was used as a loading control. (B) Antibody feeding assay for MT4-WT (green) after a 30-min incubation at 37 °C. Cell membranes were marked in red with cell tracker. (C) Computerized quantification of confocal images representing internalized MT4-WT in MDA-MB-231 cells at 30 min. The cells were observed under confocal microscope and using a 60X objective. (D) Antibody feeding assay for MT4-E249A (green) after a 30-min incubation at 37 °C. Cell membranes were marked in red with cell tracker. (E) Computerized quantification of confocal images representing cell surface MT4-E249A in MDA-MB-231 cells at 30 min. The data and statistical analysis in (D) and (E) are representative of two independent experiments ($n = 2$) performed in biological triplicates. Data are presented as the mean (± SEM), and statistical analyses were performed with Wilcoxon–Mann–Whitney tests. $*P \leq 0.05$; $****P \leq 0.0001$. (F) Western blot analysis of CDC42, Rac1 and RhoA in MT4-MMP cells incubated with CDC42, Rac1, RhoA or scrambled siRNA. Actin was used as a loading control. (G) FACS analysis of MT4-MMP levels at the cell surface (intact cells) after CDC42, Rac1, RhoA or scrambled siRNA transfection in MDA-MB-231 cells. The median fluorescence intensity (MFI) for each condition was normalized to control cells (MDA-MB-231 cells expressing empty pcDNA3-neo vector) and compared with the scrambled siRNA, which was considered to be 100%. FACS data are presented as the mean ± standard deviation of three independent experiments ($n = 3$).

cells transfected with scrambled siRNA, whereas the amount of noninternalized MT4-E249A remained high and stable at the cell surface in cells transfected with CDC42 siRNA ($P < 0.0001$).

We next extended our study to Rac1 and RhoA, and conducted fluorescence-activated cell sorting (FACS) analysis to quantify the MT4-MMP available at the cell surface. Approximately 80% downregulation was achieved with the different siRNAs against CDC42, Rac1, and RhoA (Fig. 7F). FACS analyses showed increases in MT4-MMP availability at the cell surface of ~ 28% for CDC42 siRNA, 33% for RhoA siRNA and 11% for Rac1 siRNA as compared with scrambled siRNA (Fig. 7G). Thus, MT4-MMP internalization is primarily dependent on CDC42 and RhoA, and to a lesser extent on Rac1, indicating that MT4-MMP proficiently utilizes the CLIC/GEEC pathway (rather than caveolin-dependent or clathrin-dependent pathways) for its internalization.

Discussion

Recent evidence from our team [33] and other groups [34,37,38] has assigned mitogenic, protumorigenic and prometastatic functions to MT4-MMP, and these activities rely on both proteolytic and nonproteolytic activities [24,32]. Understanding the mechanisms regulating MT4-MMP availability at the cell surface is important for interfering with this unique multifunctional GPI-bound MMP. Although many studies have focused on the internalization and recycling of MT1-MMP, the trafficking of the prometastatic MT4-MMP has not yet been described. Herein, we demonstrate that MT4-MMP is internalized and recycled to the cell surface. By using coimmunoprecipitation experiments, and nonreducing and reducing western blotting, we found that MT4-MMP forms dimers and/or oligomers. These homophilic interactions were not abrogated by either an inactivating E249A mutation in the catalytic site or inhibition with synthetic (GM6001 and BB94) or physiological (TIMP2) MMPIs. These findings demonstrate that MT4-MMP homophilic interactions are independent of its catalytic activity.

A previous study by Sohail *et al.* [36] showed that the C564S mutation is sufficient to prevent MT4-MMP dimerization, whereas the C566S mutation has minimal effects on this process. In contrast, we found that, under nonreducing SDS/PAGE conditions, the C564S and C566S mutations do not affect MT4-MMP dimerization or oligomerization. Large quantities of MT4-MMP-C564S, MT4-MMP-C566S and MT4-MMP-C564S-C566S were found in abundant monomeric (65 kDa), dimeric (130 kDa) and oligomeric (260 kDa) species. Nevertheless, the level of a 130-kDa form, found after IP of MT4-MMP-Myc and reducing western blotting against FLAG, was decreased by the C564S mutation. This 130-kDa form may correspond to MT4-MMP oligomers, whereas the dimers are detected as 65-kDa species after IP experiments. Similarly, the double mutation of C564S and C566S in the stem region of MT4-MMP reduced the formation of this 130-kDa form without completely inhibiting other homophilic interactions. These conflicting data might appear to be inconsistent with previous evidence of C564S involvement in MT4-MMP dimerization [36]. However, this inconsistency might be explained by differences in lipid raft formation and cell membrane fluidity between the MDCK cells previously used [36] and the MDA-MB-231 and COS-1 cells used here.

Our data demonstrate that only a fraction of MT4-MMP molecules contribute to the formation of covalent dimers though intermolecular disulfide bonds and suggest the existence of other noncovalent interactions. The DTT-resistant or 2-mercaptoethanol-resistant 130-kDa band might correspond to a noncovalently

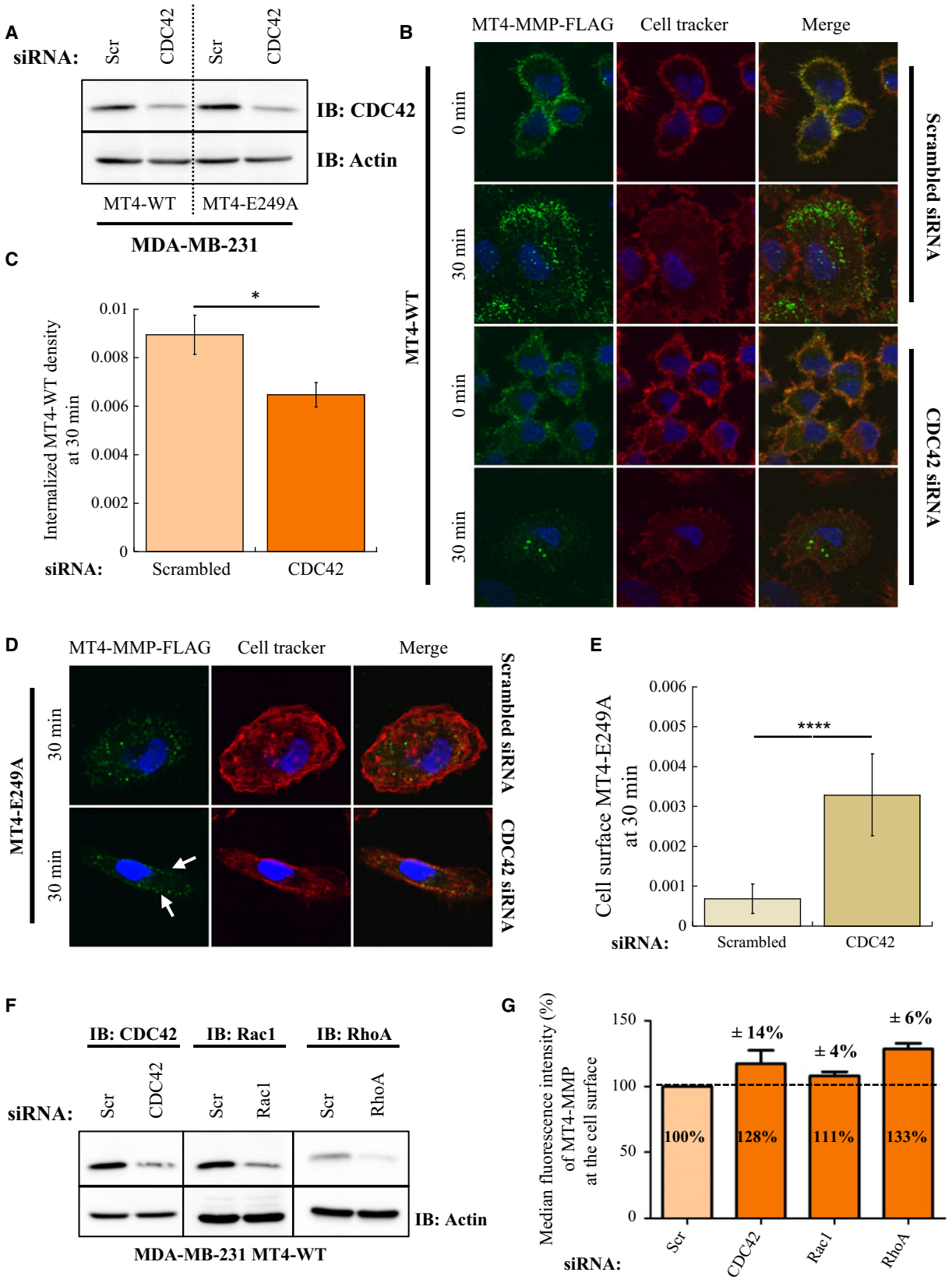
A
siRNA:
Scr
CDC42
Scr
CDC42
IB: CDC42
IB: Actin
MT4-WT
MT4-E249A
MDA-MB-231
B
MT4-MMP-FLAG
Cell tracker
Merge
0 min
30 min
0 min
30 min
MT4-WT
Scrambled siRNA
CDC42 siRNA
C
Internalized MT4-WT density at 30 min
0.01
0.008
0.006
0.004
0.002
0
*
siRNA:
Scrambled
CDC42
D
MT4-MMP-FLAG
Cell tracker
Merge
MT4-E249A
30 min
30 min
Scrambled siRNA
CDC42 siRNA
E
Cell surface MT4-E249A at 30 min
0.006
0.005
0.004
0.003
0.002
0.001
0
****
siRNA:
Scrambled
CDC42
F
IB: CDC42
IB: Rac1
IB: RhoA
siRNA:
Scr
CDC42
Scr
Rac1
Scr
RhoA
IB: Actin
MDA-MB-231 MT4-WT
G
Median fluorescence intensity (%) of MT4-MMP at the cell surface
150
100
50
0
± 14%
± 4%
± 6%
100%
128%
111%
133%
siRNA:
Scr
CDC42
Rac1
RhoA

bonded MT4-MMP dimer held by hydrophobic interactions. The detection of this band by three different antibodies excluded any artefactual species. Several studies have reported noncovalent protein–protein interactions or dimers resistant to SDS, which result in hydrophobic interactions [39–41]. Hydrophobic or polar interactions between the hemopexin domains of adjacent MT4-MMP molecules deserve more investigation to decipher their role in MT4-MMP dimerization. The presence of noncovalent interactions in MT4-MMP dimers is not surprising, as several reports have described the importance of noncovalent interactions in the oligomerization and dimerization of other MMPs, including MMP2, MMP9, and MT1-MMP, through their hemopexin domains [8,9,30]. In the case of MT1-MMP, homophilic complex formation at the cell surface requires the cooperation of two adjacent MT1-MMP molecules to cleave proMMP2 or collagen. A cysteine (Cys574) present in the cytosolic tail of MT1-MMP has been reported to be involved in its dimerization through the formation of an intermolecular disulfide bridge [28,42]. However, Itoh *et al.* have proposed that the hemopexin-like domain of MT1-MMP is responsible for homophilic complex formation [29]. In contrast, Overall *et al.* failed to detect homodimers of MT1-MMP hemopexin domains [43]. More recently, Lehti *et al.* concluded that both the hemopexin-like and cytoplasmic domains of MT1-MMP are involved in the formation of enzyme oligomers that contribute to intermolecular proteolytic events at the cell surface [30]. Subsequently, Seiki *et al.* have shown that, in addition to the hemopexin domain, MT1-MMP can form dimers through its transmembrane domain [10].

Internalization kinetic assays revealed low levels of MT4-MMP internalization after 15 min and higher levels after 45–60 min. These kinetics are slower than those of MT1-MMP, for which optimal internalization is observed after 30 min [44]. This difference in kinetics might be attributable to structural differences between the molecules, related to their membrane anchorage domains and probably to their pericellular proteolytic performances. Similarly, internalization of the GPI-anchored MT6-MMP was reported to be low as compared with that of MT1-MMP [45]. MT1-MMP has a broader repertoire of substrates than MT4-MMP, and the rapid internalization of MT1-MMP probably contributes to the control of its activity. Because of the poorer activity of MT4-MMP [46], the pericellular functions of the protein might require longer persistence at the cell surface. Furthermore, GPI-anchored proteins are known to accumulate and recycle slowly as compared with proteins that use clathrin-dependent endocytosis [47,48].

The inert MT4-E249A form was internalized at a similar rate as MT4-WT, and was found intact in cytosolic endosomes, whereas a fraction of the WT form was subjected to autodegradation. The detection of higher levels of intracellular MT4-WT upon treatment with BB94 suggests autodegradation of the protein. Once internalized, MT4-MMP was found associated with EEA1-positive endosomes. Interestingly, some MT4-MMP was recycled intact to the cell surface 30 min after its internalization. For the first time, MT4-MMP bioavailability at the cell surface has been found to be regulated through its internalization, degradation and recycling in human breast cancer cells. Through its recycling, MT4-MMP could be repeatedly used by cancer cells during invasion and metastatic dissemination.

MT1-MMP has been reported to colocalize with caveolin-coated and clathrin-coated pits at the cell surface, and to use both pathways for internalization [49]. We observed that MT4-MMP colocalized with caveolin but not with clathrin. This observation is in agreement with a previous report showing that MT4-MMP colocalizes with CAV-1 [38]. Intriguingly, MT4-MMP internalization was not inhibited by either a caveolin inhibitor or a clathrin inhibitor. We then hypothesized that an alternative pathway may be used by MT4-MMP for its internalization. Several studies have reported that the CLIC/GEEC pathway plays a role in the internalization of GPI-anchored proteins. Small Rho GTPases involved in this pathway include CDC42 and RhoA. By applying a siRNA approach, we found that CDC42 and RhoA proteins are the primary drivers of MT4-MMP internalization. In contrast, silencing Rac1 only minimally affected MT4-MMP internalization. CLIC/GEEC pathway-dependent internalization was confirmed by two approaches, including antibody feeding assays followed by computerized quantification of confocal images and FACS quantification, which showed 28% and 33% increases in the level of cell surface MT4-MMP upon CDC42 and RhoA silencing, respectively. Notably, these values do not take into account a large amount of MT4-MMP that may be shed from the cell surface or autodegraded when internalization is inhibited by the Rho GTPase siRNA. The latter was confirmed by demonstrating that CDC42 silencing in MT4-E249A cells led to its blockade at the cell surface, and that this noninternalized inert form was found intact after 30 min of incubation at 37 °C, whereas the active form was not stable under these conditions. These data indicate that MT4-MMP internalization is efficiently

inhibited by CDC42 siRNA, and that the resulting non-internalized active form of MT4-MMP is autodegraded and not available at the cell surface after 30 min.

Together, these data indicate that, in contrast to MT1-MMP, which uses clathrin and caveolin as the major endocytosis pathways, MT4-MMP endocytosis is dependent on Rho GTPases and the CLIC/GEEC pathway. The data presented here shed a new light on the cellular and biochemical characteristics of MT4-MMP, which is emerging as a prometastatic MT-MMP with unique features among other MT-MMP subfamilies.

MMPs exert their proteolytic activity and degrade substantial barriers, facilitating angiogenesis, and tumour growth, invasion, and metastasis [50,51]. However, MMPs show dual functions during cancer progression, based on their ability to: (a) degrade extracellular matrix, which allows tissue invasion; and (b) generate and/or release proangiogenic or anti-angiogenic and inflammatory mediators [52]. This dual function was pointed to as a key cause of clinical trial failure with MMPIs [19,52]. Recently, it has emerged that MMPs contribute to cancer progression and cell signalling by non-proteolytic functions dependent on a direct binding to adhesion molecules, integrins or tyrosine kinase receptors [1,2,53]. Thus, understanding how the availability of MMPs at cell surface is regulated is important, and promising for understanding the failure of some targeted therapies.

Experimental procedures

Cell culture

Human breast cancer MDA-MB-231 cells and monkey epithelial COS-1 cells were obtained from the American Type Culture Collection (ATCC, Manassas, VA, USA). All cell lines described above were authenticated before being used in experiments. Cell line authentication for interspecies contamination was performed by Leibniz-Institute DSMZ, Braunschweig, Germany. Cells were grown in Dulbecco's modified Eagle's medium (DMEM) supplemented with 10% FBS, L-glutamine (2 mM), penicillin (100 $U \cdot mL^{-1}$) and streptomycin (100 $U \cdot mL^{-1}$) at 37 °C in a 5% CO_2 humid atmosphere. All culture reagents were purchased from Gibco-Life Technologies (Invitrogen, Paisley, UK).

Transfection, plasmids, and mutagenesis

Plasmids carrying MT4-MMP were tagged by a FLAG peptide (DYKDDDDK) after Pro319 or by a Myc peptide (EQKLISEEDL) after Leu313 in the hinge region of the protease (Fig. 1A). Stable transfectants were cultured in medium containing 1.25 $mg \cdot mL^{-1}$ Geneticin (G418 sulfate; Invitrogen Life Technologies, Grand Island, NY, USA). For mutagenesis experiments, Cys564 and Cys566 in the stem region of MT4-MMP were replaced with serines (C564S and C566S, respectively) by use of the QuikChange II XL Site-Directed Mutagenesis Kit (#200521, Agilent) applied on WT pcMT4 cDNA (MT4-WT) and inactive forms of pcMT4 cDNA (MT4-E249A) containing FLAG or Myc tag (Fig. 1A). The generation of a stable MDA-MB-231 cell line expressing MT4-MMP (MT4-WT) or MT4-E249A was performed as previously described [32].

Coimmunoprecipitation assay

Coimmunoprecipitation assays were performed in COS-1 cells double-transfected with a FLAG-tagged human MT4 plasmid and a Myc-tagged human MT4 plasmid (see above). Forty-eight hours after transient transfection, total proteins were extracted with lysis buffer (50 mM Tris/HCl, pH 7.4; 150 mM NaCl; 1% Nonidet P40; 1% Triton X-100; 1% sodium deoxycholate; 0.1% SDS) containing a Protease Inhibitor Cocktail (complete; Roche). Protein lysates (500 μg) were incubated with 2 μg of antibody against Myc (M5546 or C3956; Sigma) and 50 μL of 50% slurry Dynabeads protein G (Invitrogen) to coimmunoprecipitate MT4-MMP and its protein partners. The precipitate was subjected to western blotting with a mAb against FLAG M2 (1 : 1000 dilution) (F3165; Sigma, St Louis, MO, USA) and horseradish peroxidase-conjugated secondary antibody.

In some assays, COS-1 cells were incubated with the following MMPIs 24 h before protein extraction: GM-6001 (20 μM), BB94 (20 μM), or TIMP2 (100 $ng \cdot mL^{-1}$); DMSO was used as a control.

RNA extraction and RT-PCR analysis

Total RNAs were extracted from cells at 70–80% confluence with the High Pure RNA isolation kit (Roche Diagnostic Applied Science, Mannheim, Germany). RT-PCR was performed on 10 ng of total RNA extracted from MDA-MB-231 cells with the GeneAmp Thermostable rTth Reverse Transcriptase RNA PCR kit (Applied Biosystems, Foster City, CA, USA), according to the manufacturer's instructions. Specific primers for human MT4-MMP were designed as follows: forward, 5′-AAGGAGACAGGTACTGGG TGTTC-3′; and reverse, 5′-TCGCCATCCAGCACTTTC CAGTA-3′ (Eurogentec, Seraing, Belgium). Thirty cycles of amplification were run for 15 s at 94 °C, 20 s at 68 °C, and 30 s at 72 °C.

Western blotting

Cell protein extracts were prepared in lysis buffer (50 mM Tris/HCl, pH 7.4; 150 mM NaCl; 1% Nonidet P40; 1% Tri-

ton X-100; 1% sodium deoxycholate; 0.1% SDS) containing Protease Inhibitor Cocktail (complete; Roche). Proteins were boiled for 5 min at 95 °C in loading buffer containing 2-mercaptoethanol before western blotting. In nonreducing conditions, 2-mercaptoethanol was excluded from the loading buffer. Protein samples were separated on 12% polyacrylamide gels, and transferred to poly(vinylidene difluoride) membranes (NEN, Boston, MA, USA). Membranes were blocked with 1% casein/0.1% Tween-20/PBS (or 3% milk/0.1% Tween-20/PBS), and incubated overnight with primary antibody at 4 °C, and then with a secondary horseradish peroxidase-conjugated anti-mouse Ig or anti-rabbit IgG (Cell Signaling Technology, Danvers, MA, USA). Signals were detected with an enhanced chemiluminescence kit (Perkin-Elmer Life Sciences, Boston, MA, USA). As a loading control, membranes were stripped and reincubated with an antibody against actin (1 : 1000 dilution) (A2066; Sigma) or an antibody against HSC-70 (1 : 5000) (sc7298; Santa Cruz). The primary antibodies used were: mAb against FLAG M2 (1 : 1000) (F3165; Sigma, St Louis, MO, USA); antibodies against MT4-MMP (MMP17) (1 : 1000) (ab39028 and ab51075; Abcam, Cambridge, UK); antibody against CDC42 (0.5 $\mu g \cdot mL^{-1}$, #610929; BD Transduction Laboratories, San Diego, CA, USA); antibody against Rac1 (clone 23A8, 0.5 $\mu g \cdot mL^{-1}$, #05-389; Millipore), or antibody against RhoA (26C4) (sc-418, 0.8 $\mu g \cdot mL^{-1}$; Santa Cruz Biotechnologies, Santa Cruz, CA, USA). Western blot density bands were quantified with QUANTITY-ONE software (BioRad Laboratories, Hercules, CA, USA).

Cell surface biotinylation and recycling assay

Cells were grown in 10-cm-diameter or 15-cm-diameter plates for MT4-MMP uptake and recycling assays, respectively. This protocol was adapted from Remacle *et al.* [49]. Briefly, the cells were washed twice with cold PBS, and once with Soerensen Buffer (SBS) (14.7 mM KH_2PO_4 and 2 mM Na_2HPO_4 with 120 mM sorbitol, pH 7.8), and incubated for 10 min in SBS on ice. Biotinylation of cell surface proteins was performed by adding 0.3 $mg \cdot mL^{-1}$ EZ-Link Sulfo-NHS-SS-biotin (#21331; Thermo Scientific, Waltham, MA, USA) in SBS for 20 min on ice. After several washes, the excess biotin was quenched for 10 min on ice by incubation in 100 mM glycine/SBS. After washing to remove the glycine, the cells were incubated at 37 °C in serum-free medium to allow the internalization of biotinylated plasma membrane proteins. After various times (15, 30, 45 and 60 min) of incubation at 37 °C, the uptake was stopped by washing the cells with ice-cold SBS and 10 min of incubation in SBS on ice. Biotin that remained present on cell surface proteins was removed by a 25-min incubation with 150 mM MESNA, a membrane-impermeant reducing agent (pH 8.2 in ice-cold SBS). After three washes with ice-cold SBS, cell proteins were extracted with a lysis buffer (50 mM Tris/HCl, pH 7.4; 150 mM NaCl; 1% Nonidet P40; 1% Triton X-100; 1% sodium deoxycholate; 0.1% SDS) containing Protease Inhibitor Cocktail (complete; Roche). In some assays, the cells were incubated with BB94 for 24 h before cell biotinylation. For the recycling assay, cells were incubated for 45 min at 37 °C and treated with MESNA. Next, the cells were incubated a second time at 37 °C for 30 min to allow recycling of the endocytosed biotinylated proteins at the cell surface. Biotin re-exposed at the cell surface was removed by a second MESNA treatment. Finally, the cells were washed three times with ice-cold SBS, and cell proteins were extracted with a lysis buffer as described above. Biotinylated proteins (600–800 μg) were pulled down with streptavidin–agarose beads (Sigma) overnight at 4 °C, and used for the detection of MT4-MMP by western blotting.

Immunofluorescence and confocal microscopy

MDA-MB-231 cells expressing MT4-WT or MT4-E249A were grown on 12-mm sterile round glass coverslips. After 24 h of incubation, the cells were washed with PBS and fixed for 15 min in 4% paraformaldehyde at room temperature. After being washed, the cells were permeabilized for 5 min at room temperature with 0.25% Triton X-100/PBS. The slides were blocked in PBS containing 10% BSA solution, and incubated with an antibody against FLAG (1 : 500 dilution, F1804; Sigma, St Louis, MO, USA) in 3% BSA/PBS for 2 h at 37 °C. The cells were then incubated with a secondary antibody, i.e. Alexa Fluor 488 goat anti-(mouse IgG) (1 : 1000 dilution, A11029; Invitrogen), in 3% BSA/PBS for 45 min at 37 °C, and labelled with 4′,6-diamidino-2-phenylindole dihydrochloride (D1306, 1 : 4000 dilution; Life Technologies) for 5 min at room temperature to detect nuclei. Finally, the cells were mounted on slides with Aqua-Poly/Mount Coverslipping Medium (#18600; Polysciences). To block caveolin-dependent or clathrin-dependent endocytosis, cells were incubated for 1 h in serum-free medium with filipin III (5 $\mu g \cdot mL^{-1}$ and 10 $\mu g \cdot mL^{-1}$) or chlorpromazine (5 $\mu g \cdot mL^{-1}$), respectively. For colocalization experiments, MDA-MB-231 cells expressing MT4-MMP were stained with an antibody against FLAG (see above) and an antibody against CAV-1 at 1 : 100 dilution (C13630; Transduction Lab), or with an antibody against clathrin heavy chain 1 (CHC-1) at 1 : 100 dilution (#2410; Cell Signaling). The slides were analysed on an Olympus FV1000 confocal microscope with a × 60 oil immersion objective (Olympus America, Waltham, MA, USA).

Antibody feeding assay

Cells expressing MT4-WT-FLAG or MT4-E249A-FLAG were grown on 12-mm glass coverslips for 24 h at 37 °C. The cells were washed with PBS, and incubated at 37 °C for 30 min in serum-free DMEM supplemented with L-glutamine (2 mM), penicillin (100 $U \cdot mL^{-1}$), streptomycin (100 $U \cdot mL^{-1}$),

and 5% BSA Fraction V. The cells were then washed with ice-cold DMEM and incubated for 15 min on ice. The MDA-MB-231 cells were incubated with a mouse antibody against FLAG M2 at 1 : 500 dilution (F1804; Sigma, St Louis, MO, USA) for 1 h on ice. Unbound antibodies were cleared by several washes. The cells were incubated for different times at 37 °C to allow internalization of cell surface MT4-MMP-FLAG marked by the antibody against FLAG. The cells were finally fixed with 4% paraformaldehyde, permeabilized with 0.25% Triton X-100/PBS, and incubated with a secondary antibody, i.e. Alexa Fluor 488-coupled goat anti-mouse IgG (1 : 1000, A11029; Invitrogen), for 45 min at 37 °C. For experiments assessing colocalization of MT4-MMP-FLAG and EEA1-positive early endosomes, the cells were incubated for 1 h at 37 °C with an antibody against EEA1 (ab2900; Abcam) and for 45 min at 37 °C with a secondary antibody, i.e. Alexa Fluor 546 goat anti-(rabbit IgG) (2 $\mu g \cdot mL^{-1}$, A11035; Invitrogen). For detection of nuclei, the cells were incubated with 4′,6-diamidino-2-phenylindole dihydrochloride (1 : 4000, D1306; Life Technologies) for 5 min at room temperature. In some assays, a red cell membrane tracker, DY-554-phalloidin (554-33; Dyomics) was used. Finally, the cells were mounted on slides with Aqua-Poly/Mount Coverslipping Medium (#18600; Polysciences), and confocal images were collected on an Olympus FV1000 microscope and analysed with Olympus FLUOVIEW (FV-10 ASW) software (Olympus America).

Computerized quantification of internalized and cell surface MT4-MMP in immunofluorescence experiments

Computerized image quantification was performed with the image analysis toolbox of MATLAB R2014a (8.3.0.532) (64-bit; MathWorks) applied on individual cells. Cell surface staining and intracellular staining were automatically detected, and the resulting images were binarized. Results are expressed as the mean ± standard error of the mean (SEM) of the ratio between the intracellular staining areas and the cell surface (internalized MT4-MMP density) or total cell surface staining areas in a 2-μm-thick layer of cell membrane marked with cell surface tracker in MT4-E249A-expressing cells (cell surface MT4-E249A). For statistical analysis, Wilcoxon–Mann–Whitney tests were performed. The levels of significance were: $P > 0.05$ [not significant (NS)]; $*P \leq 0.05$; $**P \leq 0.01$; $***P \leq 0.001$; and $****P \leq 0.0001$.

siRNA transfection and flow cytometry

The expression levels of CDC42, Rac1 and RhoA were downregulated by siRNA with calcium phosphate-mediated transfection. The different siRNAs were incubated in $CaCl_2$ (2.5 M) before addition of Hepes-Buffered Saline Phosphate (140 mM NaCl; 0.75 mM Na_2HPO_4; 6 mM glucose; 5 mM KCl; 25 mM Hepes, pH 7.05). MT4-FLAG-expressing MDA-MB-231 cells and control MDA-MB-231 cells were ultimately transfected with 20 nM siRNA. After 14–16 h of transfection, the cells were washed and grown in six-well plates for 24 h. The cells were then detached with Accutase, and incubated with an FITC-conjugated mAb against FLAG M2 (clone M2, F4049; Sigma) in 1% BSA/PBS for 60 min at 4 °C. After washing, nonpermeabilized cells were analysed by flow cytometry, with 10 000 events (FACSCalibur II; BD Biosciences). The median fluorescence intensity for each condition was normalized to control cells (MDA-MB-231 cells expressing empty pcDNA3-neo vector), and compared with scrambled siRNA, which was considered to be 100%. The data represent two independent experiments. The error bars correspond to the standard deviation.

Acknowledgements

This work was supported by grants from the Fonds de la Recherche Scientifique FRS-FNRS (grant FNRS FC 91822), the Fondation Contre le Cancer, the Plan Cancer, the Interuniversity Attraction Poles Programme – Belgian Science Policy, the Centre Anticancéreux (CAC) and Fonds spéciaux of the University of Liège, Belgium. We thank the imaging and flow cytometry platform of the Groupe Interdisciplinaire de Génoprotéomique Appliquée and the Laure Volders for technical support.

Author contributions

N. E. Sounni and A. Noel supervised the project. N. E. Sounni and A. Truong designed the study. A. Truong performed experiments. C. Yip and A. Paye helped with the experiments. C. Munaut designed the plasmids. C. Deroanne designed the siRNA. S. Blacher quantified the IF data. A. Truong and N. E. Sounni analysed data and discussed the results. N. E. Sounni and A. Truong wrote the manuscript.

References

1 Noel A, Albert V, Bajou K, Bisson C, Devy L, Frankenne F, Maquoi E, Masson V, Sounni NE & Foidart JM (2001) New functions of stromal proteases and their inhibitors in tumor progression. *Surg Oncol Clin N Am* **10**, 417–432. x–xi.

2 Sounni NE, Paye A, Host L & Noel A (2011) MT-MMPS as regulators of vessel stability associated with angiogenesis. *Front Pharmacol* **2**, 111.

3 Folgueras AR, Pendas AM, Sanchez LM & Lopez-Otin C (2004) Matrix metalloproteinases in cancer: from new functions to improved inhibition strategies. *Int J Dev Biol* **48**, 411–424.
4 Page-McCaw A, Ewald AJ & Werb Z (2007) Matrix metalloproteinases and the regulation of tissue remodelling. *Nat Rev Mol Cell Biol* **8**, 221–233.
5 Egeblad M & Werb Z (2002) New functions for the matrix metalloproteinases in cancer progression. *Nat Rev Cancer* **2**, 161–174.
6 Niarakis A, Giannopoulou E, Ravazoula P, Panagiotopoulos E, Zarkadis IK & Aletras AJ (2013) Detection of a latent soluble form of membrane type 1 matrix metalloprotease bound with tissue inhibitor of matrix metalloproteinases-2 in periprosthetic tissues and fluids from loose arthroplasty endoprostheses. *FEBS J* **280**, 6541–6555.
7 Hsiao CC, Wang WC, Kuo WL, Chen HY, Chen TC, Hamann J & Lin HH (2014) CD97 inhibits cell migration in human fibrosarcoma cells by modulating TIMP-2/MT1- MMP/MMP-2 activity–role of GPS autoproteolysis and functional cooperation between the N- and C-terminal fragments. *FEBS J* **281**, 4878–4891.
8 Olson MW, Bernardo MM, Pietila M, Gervasi DC, Toth M, Kotra LP, Massova I, Mobashery S & Fridman R (2000) Characterization of the monomeric and dimeric forms of latent and active matrix metalloproteinase-9. Differential rates for activation by stromelysin 1. *J Biol Chem* **275**, 2661–2668.
9 Koo BH, Kim YH, Han JH & Kim DS (2012) Dimerization of matrix metalloproteinase-2 (MMP-2): functional implication in MMP-2 activation. *J Biol Chem* **287**, 22643–22653.
10 Itoh Y, Ito N, Nagase H & Seiki M (2008) The second dimer interface of MT1-MMP, the transmembrane domain, is essential for ProMMP-2 activation on the cell surface. *J Biol Chem* **283**, 13053–13062.
11 Sounni NE, Roghi C, Chabottaux V, Janssen M, Munaut C, Maquoi E, Galvez BG, Gilles C, Frankenne F, Murphy G *et al.* (2004) Up-regulation of vascular endothelial growth factor-A by active membrane-type 1 matrix metalloproteinase through activation of Src-tyrosine kinases. *J Biol Chem* **279**, 13564–13574.
12 Eisenach PA, Roghi C, Fogarasi M, Murphy G & English WR (2010) MT1-MMP regulates VEGF-A expression through a complex with VEGFR-2 and Src. *J Cell Sci* **123**, 4182–4193.
13 Chan KM, Wong HL, Jin G, Liu B, Cao R, Cao Y, Lehti K, Tryggvason K & Zhou Z (2012) MT1-MMP inactivates ADAM9 to regulate FGFR2 signaling and calvarial osteogenesis. *Dev Cell* **22**, 1176–1190.
14 Tang Y, Rowe RG, Botvinick EL, Kurup A, Putnam AJ, Seiki M, Weaver VM, Keller ET, Goldstein S, Dai J *et al.* (2013) MT1-MMP-dependent control of skeletal stem cell commitment via a beta1-integrin/YAP/TAZ signaling axis. *Dev Cell* **25**, 402–416.
15 Pratt J & Annabi B (2014) Induction of autophagy biomarker BNIP3 requires a JAK2/STAT3 and MT1-MMP signaling interplay in Concanavalin-A-activated U87 glioblastoma cells. *Cell Signal* **26**, 917–924.
16 Sounni NE & Noel A (2005) Membrane type-matrix metalloproteinases and tumor progression. *Biochimie* **87**, 329–342.
17 Zucker S, Pei D, Cao J & Lopez-Otin C (2003) Membrane type-matrix metalloproteinases (MT-MMP). *Curr Top Dev Biol* **54**, 1–74.
18 Sohail A, Sun Q, Zhao H, Bernardo MM, Cho JA & Fridman R (2008) MT4-(MMP17) and MT6-MMP (MMP25), A unique set of membrane-anchored matrix metalloproteinases: properties and expression in cancer. *Cancer Metastasis Rev* **27**, 289–302.
19 Noel A, Gutierrez-Fernandez A, Sounni NE, Behrendt N, Maquoi E, Lund IK, Cal S, Hoyer-Hansen G & Lopez-Otin C (2012) New and paradoxical roles of matrix metalloproteinases in the tumor microenvironment. *Front Pharmacol* **3**, 140.
20 Shiryaev SA, Cieplak P, Aleshin AE, Sun Q, Zhu W, Motamedchaboki K, Sloutsky A & Strongin AY (2011) Matrix metalloproteinase proteolysis of the mycobacterial HSP65 protein as a potential source of immunogenic peptides in human tuberculosis. *FEBS J* **278**, 3277–3286.
21 Marco M, Fortin C & Fulop T (2013) Membrane-type matrix metalloproteinases: key mediators of leukocyte function. *J Leukoc Biol* **94**, 237–246.
22 D'Alessio S, Ferrari G, Cinnante K, Scheerer W, Galloway AC, Roses DF, Rozanov DV, Remacle AG, Oh ES, Shiryaev SA *et al.* (2008) Tissue inhibitor of metalloproteinases-2 binding to membrane-type 1 matrix metalloproteinase induces MAPK activation and cell growth by a non-proteolytic mechanism. *J Biol Chem* **283**, 87–99.
23 Sounni NE, Rozanov DV, Remacle AG, Golubkov VS, Noel A & Strongin AY (2010) Timp-2 binding with cellular MT1-MMP stimulates invasion-promoting MEK/ERK signaling in cancer cells. *Int J Cancer* **126**, 1067–1078.
24 Paye A, Truong A, Yip C, Cimino J, Blacher S, Munaut C, Cataldo D, Foidart JM, Maquoi E, Collignon J *et al.* (2014) EGFR activation and signaling in cancer cells are enhanced by the membrane-bound metalloprotease MT4-MMP. *Cancer Res* **74**, 6758–6770.

25 Holmbeck K, Bianco P, Yamada S & Birkedal-Hansen H (2004) MT1-MMP: a tethered collagenase. *J Cell Physiol* **200**, 11–19.
26 Sato H, Takino T, Okada Y, Cao J, Shinagawa A, Yamamoto E & Seiki M (1994) A matrix metalloproteinase expressed on the surface of invasive tumour cells. *Nature* **370**, 61–65.
27 Strongin AY, Collier I, Bannikov G, Marmer BL, Grant GA & Goldberg GI (1995) Mechanism of cell surface activation of 72-kDa type IV collagenase. Isolation of the activated form of the membrane metalloprotease. *J Biol Chem* **270**, 5331–5338.
28 Rozanov DV, Deryugina EI, Ratnikov BI, Monosov EZ, Marchenko GN, Quigley JP & Strongin AY (2001) Mutation analysis of membrane type-1 matrix metalloproteinase (MT1-MMP). The role of the cytoplasmic tail Cys(574), the active site Glu(240), and furin cleavage motifs in oligomerization, processing, and self-proteolysis of MT1-MMP expressed in breast carcinoma cells. *J Biol Chem* **276**, 25705–25714.
29 Itoh Y, Takamura A, Ito N, Maru Y, Sato H, Suenaga N, Aoki T & Seiki M (2001) Homophilic complex formation of MT1-MMP facilitates proMMP-2 activation on the cell surface and promotes tumor cell invasion. *EMBO J* **20**, 4782–4793.
30 Lehti K, Lohi J, Juntunen MM, Pei D & Keski-Oja J (2002) Oligomerization through hemopexin and cytoplasmic domains regulates the activity and turnover of membrane-type 1 matrix metalloproteinase. *J Biol Chem* **277**, 8440–8448.
31 Galvez BG, Genis L, Matias-Roman S, Oblander SA, Tryggvason K, Apte SS & Arroyo AG (2005) Membrane type 1-matrix metalloproteinase is regulated by chemokines monocyte-chemoattractant protein-1/ccl2 and interleukin-8/CXCL8 in endothelial cells during angiogenesis. *J Biol Chem* **280**, 1292–1298.
32 Host L, Paye A, Detry B, Blacher S, Munaut C, Foidart JM, Seiki M, Sounni NE & Noel A (2012) The proteolytic activity of MT4-MMP is required for its pro-angiogenic and pro-metastatic promoting effects. *Int J Cancer* **131**, 1537–1548.
33 Chabottaux V, Sounni NE, Pennington CJ, English WR, van den Brule F, Blacher S, Gilles C, Munaut C, Maquoi E, Lopez-Otin C *et al.* (2006) Membrane-type 4 matrix metalloproteinase promotes breast cancer growth and metastases. *Cancer Res* **66**, 5165–5172.
34 Rizki A, Weaver VM, Lee SY, Rozenberg GI, Chin K, Myers CA, Bascom JL, Mott JD, Semeiks JR, Grate LR *et al.* (2008) A human breast cell model of preinvasive to invasive transition. *Cancer Res* **68**, 1378–1387.
35 Shay G, Lynch CC & Fingleton B (2015) Moving targets: emerging roles for MMPs in cancer progression and metastasis. *Matrix Biol* **44–46**, 200–206.
36 Sohail A, Marco M, Zhao H, Shi Q, Merriman S, Mobashery S & Fridman R (2011) Characterization of the dimerization interface of membrane Type 4 (MT4)-matrix metalloproteinase. *J Biol Chem* **286**, 33178–33189.
37 Huang CH, Yang WH, Chang SY, Tai SK, Tzeng CH, Kao JY, Wu KJ & Yang MH (2009) Regulation of membrane-type 4 matrix metalloproteinase by SLUG contributes to hypoxia-mediated metastasis. *Neoplasia* **11**, 1371–1382.
38 Nimri L, Barak H, Graeve L & Schwartz B (2013) Restoration of caveolin-1 expression suppresses growth, membrane-type-4 metalloproteinase expression and metastasis-associated activities in colon cancer cells. *Mol Carcinog* **52**, 859–870.
39 Fatemi SH & Folsom TD (2014) Existence of monomer and dimer forms of mGluR5, under reducing conditions in studies of postmortem brain in various psychiatric disorders. *Schizophr Res* **158**, 270–271.
40 Tulumello DV & Deber CM (2009) SDS micelles as a membrane-mimetic environment for transmembrane segments. *Biochemistry* **48**, 12096–12103.
41 Atwood CS, Perry G, Zeng H, Kato Y, Jones WD, Ling KQ, Huang X, Moir RD, Wang D, Sayre LM *et al.* (2004) Copper mediates dityrosine cross-linking of Alzheimer's amyloid-beta. *Biochemistry* **43**, 560–568.
42 Kazes I, Elalamy I, Sraer JD, Hatmi M & Nguyen G (2000) Platelet release of trimolecular complex components MT1-MMP/TIMP2/MMP2: involvement in MMP2 activation and platelet aggregation. *Blood* **96**, 3064–3069.
43 Overall CM, Tam E, McQuibban GA, Morrison C, Wallon UM, Bigg HF, King AE & Roberts CR (2000) Domain interactions in the gelatinase A.TIMP-2.MT1-MMP activation complex. The ectodomain of the 44-kDa form of membrane type-1 matrix metalloproteinase does not modulate gelatinase A activation. *J Biol Chem* **275**, 39497–39506.
44 Remacle AG, Rozanov DV, Baciu PC, Chekanov AV, Golubkov VS & Strongin AY (2005) The transmembrane domain is essential for the microtubular trafficking of membrane type-1 matrix metalloproteinase (MT1-MMP). *J Cell Sci* **118**, 4975–4984.
45 Radichev IA, Remacle AG, Shiryaev SA, Purves AN, Johnson SL, Pellecchia M & Strongin AY (2010) Biochemical characterization of the cellular glycosylphosphatidylinositol-linked membrane type-6 matrix metalloproteinase. *J Biol Chem* **285**, 16076–16086.
46 English WR, Puente XS, Freije JM, Knauper V, Amour A, Merryweather A, Lopez-Otin C & Murphy G (2000) Membrane type 4 matrix metalloproteinase (MMP17) has tumor necrosis factor-alpha convertase

activity but does not activate pro-MMP2. *J Biol Chem* **275**, 14046–14055.
47 Chatterjee S, Smith ER, Hanada K, Stevens VL & Mayor S (2001) GPI anchoring leads to sphingolipid-dependent retention of endocytosed proteins in the recycling endosomal compartment. *EMBO J* **20**, 1583–1592.
48 Maeda Y & Kinoshita T (2011) Structural remodeling, trafficking and functions of glycosylphosphatidylinositol-anchored proteins. *Prog Lipid Res* **50**, 411–424.
49 Remacle A, Murphy G & Roghi C (2003) Membrane type I-matrix metalloproteinase (MT1-MMP) is internalised by two different pathways and is recycled to the cell surface. *J Cell Sci* **116**, 3905–3916.
50 Murphy G & Nagase H (2011) Localizing matrix metalloproteinase activities in the pericellular environment. *FEBS J* **278**, 2–15.
51 Brezillon S, Pietraszek K, Maquart FX & Wegrowski Y (2013) Lumican effects in the control of tumour progression and their links with metalloproteinases and integrins. *FEBS J* **280**, 2369–2381.
52 Gialeli C, Theocharis AD & Karamanos NK (2011) Roles of matrix metalloproteinases in cancer progression and their pharmacological targeting. *FEBS J* **278**, 16–27.
53 Hadler-Olsen E, Fadnes B, Sylte I, Uhlin-Hansen L & Winberg JO (2011) Regulation of matrix metalloproteinase activity in health and disease. *FEBS J* **278**, 28–45.